
Article:
Candan, F. orcid.org/0000-0002-0803-610X, Beke, A., Mahfouf, M. orcid.org/0000-0002-7349-5396 et al. (1 more author) (2024) A real-time fuzzy interacting multiple-model velocity obstacle avoidance approach for unmanned aerial vehicles. Journal of Intelligent & Robotic Systems, 110 (2). 61. ISSN 0921-0296

https://doi.org/10.1007/s10846-024-02075-6

Journal of Intelligent & Robotic Systems (2024) 110:61
https://doi.org/10.1007/s10846-024-02075-6

REGULAR PAPER

A Real-time Fuzzy Interacting Multiple-Model Velocity Obstacle Avoidance Approach for Unmanned Aerial Vehicles

Fethi Candan[1] · Aykut Beke[2] · Mahdi Mahfouf[1] · Lyudmila Mihaylova[1]

Received: 5 May 2023 / Accepted: 20 February 2024

Abstract
This paper presents a new fuzzy interacting multiple-model velocity obstacle (FIMVO) approach for collision avoidance of unmanned aerial vehicles (UAVs). The proposed approach adopts in one framework the advantages of geometric collision avoidance approaches, namely of the velocity (VO), reciprocal velocity (RVO), and hybrid reciprocal velocity obstacle (HRVO) avoidance approaches combined with fuzzy logic. This leads to a combined decision-making rule, with real-time efficiency. The developed approach is compared with geometric conventional velocity obstacle avoidance approaches: VO, RVO, and HRVO avoidance approaches. The proposed approach is carefully evaluated and validated in a simulation environment and over real UAVs. The case study includes three mini UAVs and a human teleoperator who can control only one of them. The other UAVs used the computer-based teleoperator with the proposed and compared approaches. The performance criteria have been defined in four parts: trajectory smoothness, task performance, algorithm simplicity, and reliability. In 1000 independently repeated simulations, the performance results showed that the proposed FIMVO approach was 10 times better than the VO approach in terms of the number of avoided collisions. The statistical analysis demonstrates that the proposed FIMVO approach outperforms geometric velocity obstacle avoidance approaches concerning reliability and real-time efficiency.

Keywords Unmanned aerial vehicles (UAVs) · Swarm of UAVs · Velocity obstacle avoidance approaches · Unmanned air vehicles · Fuzzy control · Collision avoidance

1 Introduction

Unmanned aerial and unmanned ground vehicles (UAVs and UGVs) have been subject to intensive research and developments since they offer effective solutions in many areas such as search and rescue, defence, aerial inspections [1], and surveillance [2]. However, unmanned and uncrewed vehicles face several challenges, especially with respect to swarm UAV control, path planning and collision avoidance. Considering the control part, linear and nonlinear controllers have been developed and implemented in many different types of UAVs [3]. Proportional-integral-derivative (PID), linear quadratic regulator - linear quadratic Gaussian (LQR-LQG) [4], fuzzy PID (FPID) [5], interval type-2 fuzzy PID (IT2-FPID) [6], model predictive control (MPC) [7] and neural network based controller [8, 9] can be given as examples for that.

Considering multi-agent systems (MAS) or swarms, observation and path planning are other challenging problems [10], especially when swarms of UAVs need to perform a mission in unknown environments. Path planning algorithms can be changed for different tasks with static and/or dynamic obstacles, and each agent/UAV can be defined as an obstacle to each other. The individual UAV velocity or UAV local path points may vary to avoid a collision. This paper focuses on the topic of collision avoidance in real-time systems.

Several velocity obstacle avoidance approaches have been developed for swarm or MAS such as the potential field

✉ Fethi Candan
fethicandan@gmail.com

Aykut Beke
abeke@aselsan.com.tr

Mahdi Mahfouf
m.mahfouf@sheffield.ac.uk

Lyudmila Mihaylova
l.s.mihaylova@sheffield.ac.uk

[1] Automatic Control and Systems Engineering, University of Sheffield, Sheffield S1 3JD, UK

[2] Department of Control Systems Design, ASELSAN, Ankara 06750, Turkey

Published online: 15 April 2024

and geometric, velocity obstacle avoidance approaches [11–14]. In this paper, we consider velocity obstacle avoidance approaches. There are two main types of geometric-based velocity obstacle approaches cooperative and non-cooperative [15, 16].

Both types of approaches often assume knowledge of each object's geometry. Suitable collision avoidance approaches perform on the assumption that there is an implicit, autonomous communication layer that allows any actor to express their purpose to another freely. The agent's aim is only partially known in non-cooperative techniques, which only use the kinematic parameters that may be inferred from the agent's onboard tracking system. In [13, 14, 17], conventional approaches such as conventional velocity obstacle (VO), reciprocal velocity obstacle (RVO), hybrid reciprocal velocity obstacle (HRVO) avoidance and optimal reciprocal collision avoidance (ORCA) have been simulated and compared to each other on MAS. In [18], a three-dimensional velocity obstacle avoidance has been designed for fixed-wing-based UAVs. By manipulating the vehicle's velocity vector in response to the geometry of the encounter, The velocity obstacle avoidance technique, a three-dimensional (3-D) version of the approach, has the ability to design an avoidance manoeuvre proactively. The results of a validation using Monte Carlo simulations in challenging super conflict scenarios show that none of the 25,000 samples had collisions. In another paper about obstacle avoidance approach [19], The Pythagorean Hodograph (PH) curve trajectory re-planning serves as an illustration for the investigation of the 3-D direct obstacle avoidance technique in dynamic space. The simulation results demonstrate that the suggested approach's ability to implement obstacle avoidance trajectory re-planning substantially as an online and it improves the flexibility of obstacle avoidance manoeuvre. Unlike 3-D velocity obstacle avoidance approaches, we focused on VO, RVO, and HRVO, directly. Next section, its formulation and its geometric figures will be explained deeply.

The main contributions of this paper are the following: 1) a new approach for UAV collision avoidance called Fuzzy Interacting Multiple-Model Velocity Obstacle Avoidance Approach (FIMVO) is proposed. The approach adopts in one framework the advantages of geometric collision avoidance approaches such as the VO, RVO, and HRVO within a fuzzy interaction decision-making logic. 2) This approach has been thoroughly tested over both simulated data and with DJI Edu UAV in real-time tasks. The relative distances of the agents/UAVs are measured for FIMVO because the system's decision and weightings of the calculated velocities are based on relative distance criteria for these multi-model velocity obstacle avoidance approaches. With the HRVO approach, UAVs/agents can determine the optimal and best velocity among VO, RVO and HRVO selected and then selected weights taken. The chosen evaluation performance criteria show that the developed approach provides a smooth trajectory, accurate real-time task performance accomplishment, algorithm simplicity and reliability.

The rest of this paper is organised as follows. Sections 2 and 3 describe the approaches of velocity obstacle avoidance as preliminary work and the proposed approach. Moreover, the simulation results for comparison and the proposed approaches are also shown in Section 4. Then, Real-time experimental results are given in Section 5. After that, a thorough evaluation and validation of this proposed approach are given. Finally, Section VI presents the conclusions and future work.

2 Geometric Collision Avoidance Approaches

This section describes briefly three of the most popular geometric velocity obstacle avoidance approaches, namely the VO, RVO, and HRVO avoidance approaches [14, 20]. Figure 1 shows the main idea behind such methods. It is illustrated for two UAVs, with their safety regions and respective velocity vectors of the UAVs.

2.1 The Classical Velocity Obstacle Avoidance Approach

Conventional velocity obstacle avoidance approaches rely on the so-called Collision Cone (CC) directly. It is described in detail in [21]. In this project, we focused on the UAV's 2-D local plane (XY). In Fig. 1, the geometrically relative position ($\lambda_{\alpha\beta}$) of the obstacle, defined radius r_c of obstacle, and the

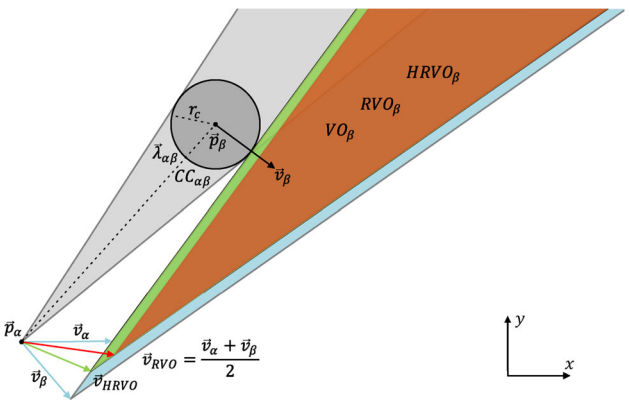

Fig. 1 The geometric-based velocity obstacle avoidance approaches

velocity vector $\mathbf{v}_\beta$ are used to generate the collision cone for obstacle β as $CC_{\alpha\beta}$. Moreover, $\mathbf{p}_\beta$ is represented as a planar cross-section centre

$$\mathrm{VO}_{\alpha\beta} = \mathrm{CC}_{\alpha\beta} \oplus \mathbf{v}_\beta. \tag{1}$$

where the classical velocity obstacle avoidance formula is written by using the Minkowski Sum ($\oplus$). the numerous number (n) of velocities $\mathrm{VO}_{1:n}$ is taken into account while considering multiple-model obstacle avoidance. Therefore, agent velocities are regarded as acceptable if $\mathbf{v}_{\alpha,k+1} \notin \mathrm{VO}_k = \cup_{\beta=1}^{n} \mathrm{VO}_{\beta,k}$ in [21]. In the existence of obstacles $\mathrm{VO}_{\beta=1:n}$ for current time $k = t_k$, velocities respecting this restriction define a collision-free track for each agent α.

2.2 The Reciprocal Velocity Obstacle Avoidance Approach

Considering the classical VO approach, RVO creates smoother avoidance trajectories in each iteration. In [22], it makes an effort to take the reciprocal velocity of the subsequent decision-making agent β into account; also, in Fig. 1, the RVO approach is shown and in Eq. 2, the RVO formula is written.

$$\mathbf{v}_{\alpha,k+1} \notin CC_{\alpha\beta} \oplus (\mathbf{v}_{\alpha,k} + \mathbf{v}_{\beta,k})/2. \tag{2}$$

Unlike VO, the created VO for each agent is defined as an enhanced apex by the mean of the agent and object velocities in RVO. The RVO at time $k = t_k$ depicts the area of velocities for α that is equal to the sum of the velocities of agent α and obstacle β. With the help of this idea, the agent may successfully follow the safer trajectory $\mathbf{v}_{\alpha,k+1}$ in line with $\mathbf{v}_\beta$ when compared to the traditional VO.

2.3 The Hybrid Reciprocal Velocity Obstacle Avoidance Approach

By enhancing the VO and RVO areas, a solution to the VO problem has been presented to eliminate the reasons for reciprocal dance. In order to evaluate various behaviours based on the relative velocity of the obstacle $\mathbf{v}_\beta$, the HRVO, as illustrated in Fig. 1, modifies the apex of the HRVO. Since the origin lines of VO_β and RVO_β are co-linear, the agent should resolve a trajectory $\mathbf{v}_{\alpha,k+1}$ to pass the obstacle on the left if it is going to the right, and vice versa. Inaction results in the phenomenon of reciprocal dancing.

Theoretically, the approach cannot ensure the development of smooth avoidance trajectories, despite evidence to the contrary in [20]. In the illustration shown in Fig. 1, the directional bias is created by changing the RVO_β's apex to be the point where the RVO_β's leading edge and VO_β's trailing edge connect, for example, $\mathrm{HRVO}_\beta = CC_{\alpha\beta} \oplus \mathbf{v}_{\mathrm{HRVO}}$. The constraint set that is subsequently placed on agent α at current time $k = t_k$ is thus expressed as $\mathbf{v}_{\alpha,k+1} \notin \mathrm{HRVO}_k = \bigcup_{\beta=1}^{n} \mathrm{HRVO}_{\alpha,k}$ in [20, 23]. The VO and A_β for obstacles O_β are:

$$\mathbf{v}_{\alpha,k} \notin \mathrm{HRVO}_k = \bigcup_{A_\beta=1}^{n} \mathrm{HRVO}_{A_\beta} \cup \bigcup_{O_\beta=1}^{n} \mathrm{VO}_{O_\beta}. \tag{3}$$

The RVO and HRVO are often only required for computing inter-agent avoidance trajectories. Instead, the union of the reciprocal variants (RVO or HRVO) for the surrounding agents can be used to represent the global VO set for agent α.

3 Fuzzy Interacting Multiple-Model Velocity Obstacle Avoidance Approach

In this study, we have designed the new FIMVO for a bounded experimental environment as shown in Figs. 11, 12, 13, and 14. The FIMVO mechanism is constructed by choosing its inputs as the absolute relative distances of the UAVs and obstacles with respect to each other, as illustrated in Fig. 2. These absolute relative distances are the distances between UAVs and the obstacle are defined as in the following:

$$\begin{aligned} \widetilde{D1} &= \sqrt{(x_1 - x_2)^2} + \sqrt{(y_1 - y_2)^2}, \\ \widetilde{D2} &= \sqrt{(x_1 - x_o)^2} + \sqrt{(y_1 - y_o)^2}, \\ \widetilde{D3} &= \sqrt{(x_2 - x_o)^2} + \sqrt{(y_2 - y_o)^2}, \end{aligned} \tag{4}$$

where, (x_1, y_1), (x_2, y_2) and (x_o, y_o) represent the locations of the UAV1, UAV2 and obstacle in 2-D plane, respectively. The universe of discourse of the antecedents membership functions (MFs) of FIMVO are defined in between [0, 1], thus the inputs ($\widetilde{D1}$, $\widetilde{D2}$ and $\widetilde{D3}$) of the FIMVO are scaled into the universe of discourse as follows:

$$\begin{aligned} D1 &= \widetilde{D1} * K_s^1, \\ D2 &= \widetilde{D2} * K_s^2, \\ D3 &= \widetilde{D3} * K_s^2, \end{aligned} \tag{5}$$

where, K_s^1 and K_s^2 are the scaling factors for the relative distances D1, D2 and D3. In summary, the FIMVO uses the absolute relative distances of the UAVs and obstacles with respect to each other to decide the best obstacle avoidance approach among the employed approaches in this work. The

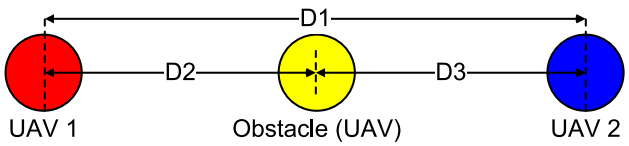

Fig. 2 Distance-based decision making

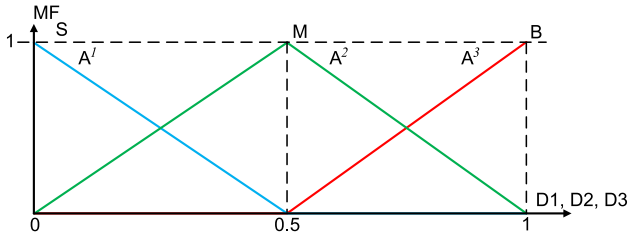

Fig. 3 Fuzzy membership functions

rule base of the FIMVO has been designed through expert knowledge and by taking into account the boundaries and limitations of the experimental environment. The rule structures of the mechanism are constructed as follows:

$$R_q: \quad \textbf{If } (D1 \; is \; A_1^i) \textbf{ and } (D2 \; is \; A_2^j) \textbf{ and } (D3 \; is \; A_3^k) \quad \textbf{Then } \alpha_1 = o_1^q, \; \alpha_2 = o_2^q \tag{6}$$

where $q : 1, ..., M(M = 27)$ is the rule number index, and M is the total rule number of the FIMVO. Here, the antecedent parts of the rule (A_1^i, A_2^j, A_3^k ; $i = 1, 2, 3, \quad j = 1, 2, 3, \quad k = 1, 2, 3$) defined with triangular MFs while o_q^1 and o_q^2 are the parameters of the consequent MFs.

As seen in Fig. 3, the antecedent MFs are specified using symmetrical triangular MFs that are uniformly distributed. Moreover, the linguistic fuzzy variables are defined as Small (S), Medium (M), and Big (B). The consequent parts ($o_{(.)}^1$, $o_{(.)}^2$) of the rules are specified using crisp singletons that correspond to the three velocity obstacle avoidance approaches that are used (VO: 1, RVO: 2, HRVO: 3). The implemented FIMVO uses and employs the product implication and the centre of sets defuzzification approach [6, 24, 25].

Remark 1 It should be noted that all antecedent MFs for the D1, D2, and D3 selected same as shown in Fig. 3. In a similar way, the consequent MFs ($o_{(.)}^1$, $o_{(.)}^2$) of the FIMVO are the same as illustrated in Fig. 4.

The outputs of FIMVO (α_1, α_2) represent the fuzzy interacting value for each velocity obstacle avoidance approach (VO, RVO, and HRVO). Moreover, $\upsilon_{(.)}$ denotes the output

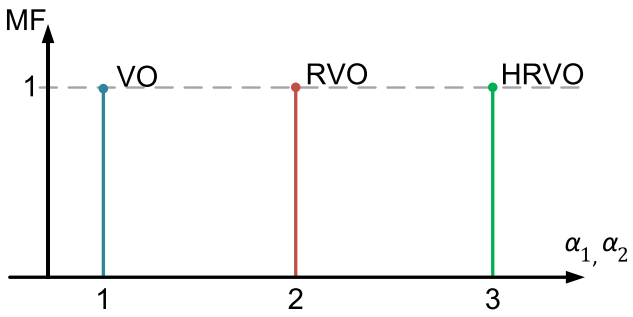

Fig. 4 Consequents of the FIMVO

velocities of fuzzy-based VO approaches. Thus, we proposed and designed an algorithm, given in Algorithm 1, that combines implemented velocity obstacle avoidance approaches which can be defined as multi-model velocity obstacle avoidance approaches. In other words, the combining mechanism acts like a type of filter by weighing the implemented velocity obstacle avoidance approaches in a factor of $\alpha_m, m \in 1, 2$.

Algorithm 1 Algorithm for combining mechanism.

if $\alpha > 2$ **then**
  $\overrightarrow{\upsilon}_{\text{FIMVO}} = (3 - \alpha)\overrightarrow{\upsilon}_{\text{RVO}} + (\alpha - 2)\overrightarrow{\upsilon}_{\text{HRVO}}$
else if $\alpha < 2$ **then**
  $\overrightarrow{\upsilon}_{\text{FIMVO}} = (2 - \alpha)\overrightarrow{\upsilon}_{\text{VO}} + (\alpha - 1)\overrightarrow{\upsilon}_{\text{RVO}}$
else
  $\overrightarrow{\upsilon}_{\text{FIMVO}} = \overrightarrow{\upsilon}_{\text{RVO}}$
end if

Remark 2 It should be noted that the same algorithm is used for both agents/UAVs.

4 Simulation and Real-Time Experimental Results

Simulation tests and real-time experiments have been done. Both simulation and real-time experiments are done on 2D Cartesian coordinates. For this reason, in real-time experiments, the altitude distance of the UAV has been set, and it is defined as $50cm$. Moreover, the heading angle (ψ) of the UAV has been also set $\psi = 0°$. The UAV mathematical model and specification of the UAV have been explained deeply. For simulation experiments, used agent/UAV model has been defined and tested. The parameters of the proposed and compared approaches have been selected with the same values and used in the simulation and real-time systems. For both experiments, the proposed and compared obstacle avoidance approaches have been performed in a Python 3.9 environment on a laptop computer running a 64-bit Windows 11 operating system with a 2.60 GHz Intel i7-10750H CPU processor. Moreover, the sampling time is the same both in the real-time experiments and in the simulations since the same latency assumption in the communication between the UAV and the computer.

4.1 Simulation Experiments

In this part, the robot model and one of the results for each velocity obstacle avoidance approach have been represented. After that, 1000 times independent repeated performance results, in terms of collision counts and task performance time, have been tabulated. A simple holonomic robot kinematic model has been used for each agent/UAV instead of

using a complex UAV model. The simple holonomic kinematic model for each agent is represented as:

$$\begin{bmatrix} x_t \\ y_t \end{bmatrix} = \begin{bmatrix} x_{t-1} \\ y_{t-1} \end{bmatrix} + \begin{bmatrix} v(x)_t \Delta t \\ v(y)_t \Delta t \end{bmatrix}, \tag{7}$$

where x_t and y_t are current position coordinates of the agent at time t, x_{t-1} and y_{t-1} denote the respective coordinates at a previous time $t-1$. The velocities of the agent are $v(x)_t$ and $v(y)_t$, respectively. The sampling time (Δt) of the UAV has been set up as 0.05s. Moreover, in the equation above, the heading angle has not been defined because it has been set to 0 and has not changed for the whole process. Therefore, it has not been added to the kinematic model.

Remark 3 Throughout the paper, agent and UAV have the same meaning. In the simulation tests, noise and disturbances have been neglected. The green star ($\star$) in the simulation is defined as the goal points of the agents. Moreover, all simulations are performed on Python environment [26].

In Fig. 5, the velocity obstacle avoidance simulation result can be seen. The total task time is 7.5 sec, and agents are close to each other. It can increase the collision possibility.

In Fig. 6, RVO avoidance approach results are presented. The results of RVO show that it has done more manoeuvre than conventional one. The total task time of RVO has been measured as 9.2 sec.

Figure 7 shows the trajectories for each UAV. The total task time of HRVO has been found to be 13.6 sec. Red and Blue agents have shown manoeuvre motion when facing static and dynamic obstacles simultaneously. For this reason, computation time has increased to avoid collision cone area.

Compared with VO, RVO, and HRVO, agents with FIMVO have smooth trajectory results, and the proposed novel method has 8.9 sec total time. The FIMVO method shows less manoeuvred motion than HRVO, and it has a better safe collision-free trajectory than RVO. However, the proposed method, FIMVO, is not faster than VO, but it has many advantages, which aforementioned before (Fig. 8).

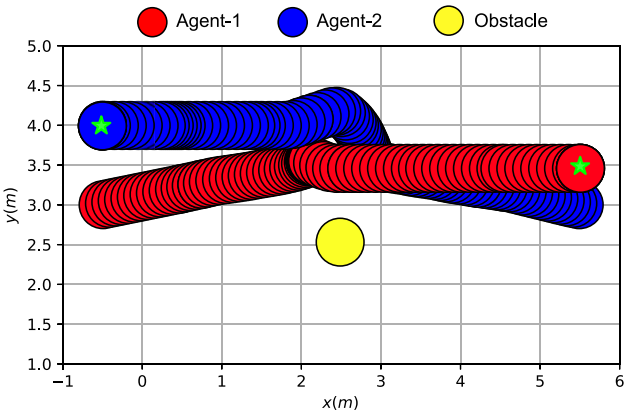

Fig. 6 Simulation result of the RVO avoidance approach

In Table 1, 1000 times independent simulation results of the proposed and compared velocity obstacle avoidance approach results are shown. It is seen that the highest number of collisions belongs to VO, but the fastest one is still VO. FIMVO, the proposed method, has significant results in terms of total collision and task performance time. The proposed method, FIMVO, has the least number of collisions. Moreover, the computation times gap between VO and FIMVO are negligible values; they are 0.001s and 0.0023s, respectively. The multiple agent experiments are presented in Appendix A.

4.2 Real-time Experiments

For the real-time testing, three DJI Tello UAVs have been used; the UAV [27] and its coordinates can be seen in Fig. 9. It is possible to calculate the conversion from the inertial

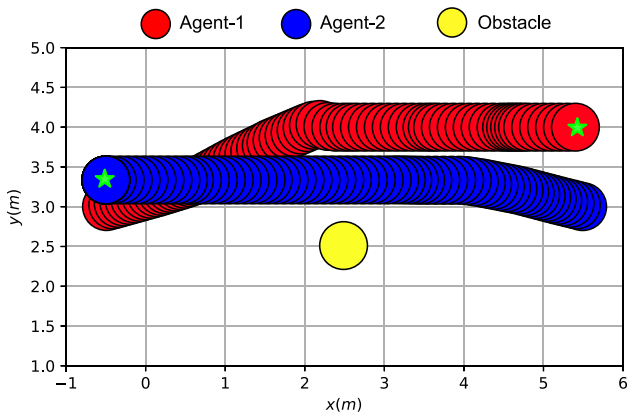

Fig. 5 Simulation result of the VO avoidance approach

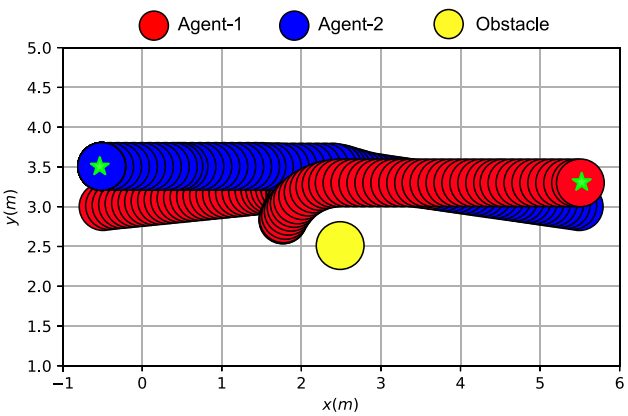

Fig. 7 Simulation result of the HRVO avoidance approach

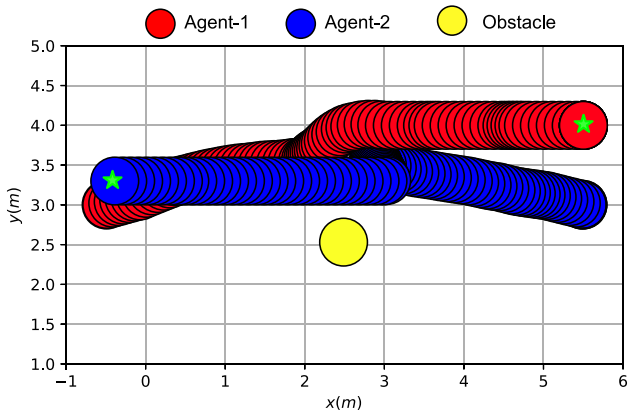

Fig. 8 Simulation result of the FIMVO avoidance approach

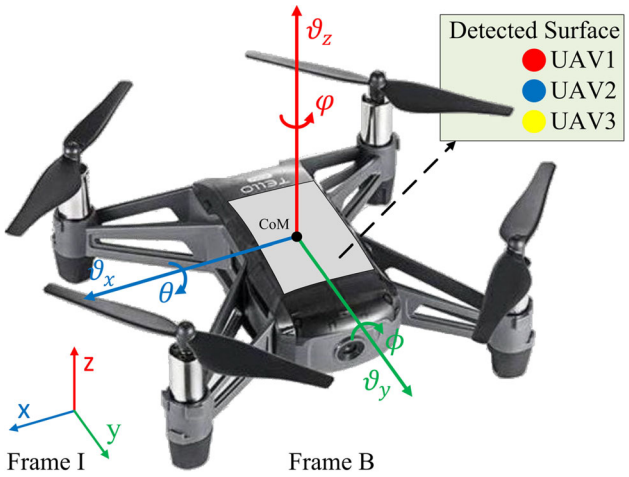

Fig. 9 The DJI Tello UAV used in the implementation

frame to the body frame or vice versa using transformation and rotation matrices. Moreover, linear velocities and attitude angles are represented as $[\upsilon_x, \upsilon_y, \upsilon_z]$ and $[\phi, \theta, \psi]$, respectively. Each UAV is designed like a holonomic robot; therefore heading angle of each UAV (ψ) has been fixed, and it is $\psi = 0$. The detected surface is coloured for each top side of the UAV (in red, blue, and yellow, respectively).

In Eq. 8, a dynamical model of the UAV has been written. In this study, we directly focused on velocity obstacle avoidance approaches; therefore, internal models and controllers have not been explained. Furthermore, controller inputs of the UAVs have been defined as linear velocities. In the equation, T, m and g denote thrust from UAV rotors, the mass of the system and gravity acceleration, respectively.

$$\begin{bmatrix} \ddot{x} \\ \ddot{y} \\ \ddot{z} \end{bmatrix} = \begin{bmatrix} \dot{\upsilon}_x \\ \dot{\upsilon}_y \\ \dot{\upsilon}_z \end{bmatrix} = \frac{\mathrm{T}}{m} \begin{bmatrix} \cos(\phi)\cos(\psi)\sin(\theta) + \sin(\phi)\sin(\psi) \\ \cos(\phi)\sin(\psi)\sin(\theta) - \cos(\psi)\sin(\phi) \\ \cos(\phi)\cos(\theta) \end{bmatrix} - \begin{bmatrix} 0 \\ 0 \\ g \end{bmatrix} \quad (8)$$

Remark 4 The dynamical model of the UAV has been designed as decoupled instead of creating highly-coupled dynamics. Due to the UAV size and weight, the coupled dynamics problems can be eliminated.

The detailed models of the DJI Tello UAV and designed controller are described in [5, 28]. Briefly, a Fuzzy PID (FPID) controller has been used, and controller parameters have been found using the "Big-Bang Big-Crunch" optimisation method. FPID and conventional controller methods have been tested and compared with each other [5, 29]. After that, it shows that FPID can guarantee stability. That means when the system faces errors such as collision or out-of-reference trajectory problems, it has existed from the position estimation or velocity obstacle avoidance approaches. Moreover, selected FPID controller parameters have been $K_e = 0.019$, $K_d = 0.0019$, $K_0 = 0.0001$, and $K_1 = 30$, respectively. The detailed structure of the FPID and the implementation has been explained in [5]. The sampling time for the real-time system has been chosen as 0.05s. The designed model and controller are the same for all UAVs. The properties of the used UAVs for experiments have been shown in Table 2.

An Intel realsense depth camera [30] with a testing area provides the testing facilities (shown in Fig. 10) for observing and localising the UAVs. Intel realsense depth camera has shown high precision results in terms of resolution, object detection and position detection. In this figure, the camera has been mounted on top of the floor, and some trigonometric formulation has been used. In [5], it has been explained and detailed intensely.

In the figure above, the positions of the UAVs have been defined as x_i, y_i and i is the number of the UAVs. Compared with the simulation experiments, the proposed and compared approaches have faced different challenging problems, such as observation noise for positioning, affecting propeller torques between each other, and centralised-based velocity obstacle avoidance calculation. In this study, position data

Table 1 Total 1000 Monte-Carlo simulation test results

Method	Total collision counts	Mean of task performance time (s)
VO	692	8.58
RVO	347	13.67
HRVO	128	15.64
FIMVO	68	11.73

Table 2 DJI Tello UAV specifications

Parameters	Value
Number of UAVs	3
UAV dimension	98 × 92 mm
Time of flight	10 min
Maximum linear velocity	[−8, 8] m/s
Boundry linear velocity	[−12, 12] %
Boundry linear velocity	[−12, 12] %

come from the Intel realsense camera as the measurement distances of UAVs.

In order to increase the challenge of the problem and to test the answers of velocity obstacle approaches under this difficulty, noises were added to the position's data, and the state estimation method was applied. In Eq. 9,

$$\omega \sim \mathcal{N}(0, 25^2) \tag{9}$$

the added noise to each UAV position has been represented to increase the challenge of the velocity approaches' comparison. Performance criteria which are trajectory smoothness, reliability, algorithm simplicity and task performance, have been directly related to velocity obstacle avoidance approaches, controller and position detection. Considering performance criteria, controller and observation effects have been minimised by using previous work [5] and a high-accuracy depth camera system [30]. Before the test in real-time, position error tolerance from the depth camera has been measured, and it has been determined as ±50 mm. After the collected raw position data from UAVs, the maximum correntropy Kalman filter (MCKF) was applied to get high accuracy on the position estimation. Detailed mathematical explanations and application results have been found in [31–33].

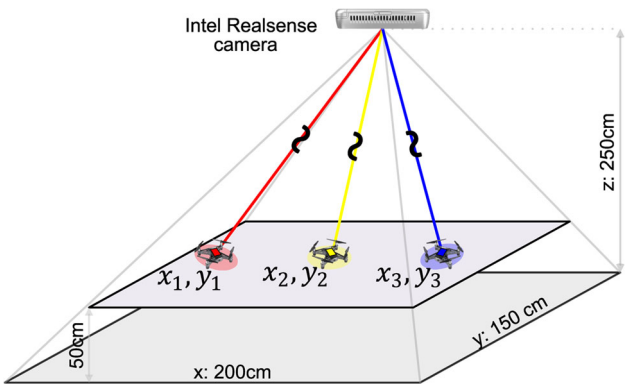

Fig. 10 Global camera location and positions of the UAVs

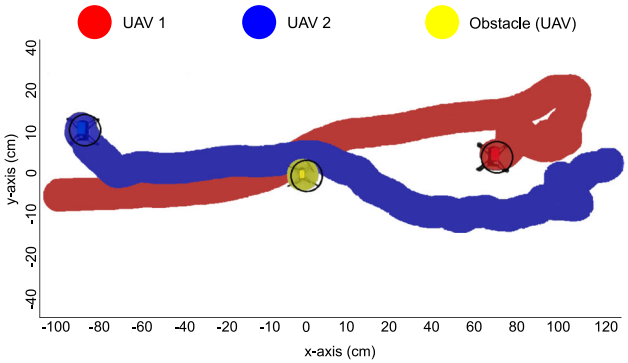

Fig. 11 The VO results for UAVs in real-time

The noise level has been between intermediate-level heavy-tailed and approximate Gaussian distributions. The heavy-tailed levels of distribution are variable between 50 and 100, monotonously. Detailed information about heavy-tailed and non-Gaussian distributions has been given in [33–35].

In the real-time tests, the proposed and compared velocity obstacle avoidance approaches have to overcome static and dynamic obstacle problems and noised sensor measurement problems even if the measurement data is filtered. In order to make a significant performance comparison of the approaches, all real-time experiments have been run ten times independently. To compare the approaches, desired velocities, which are generated from VO approaches, and collision-free positions have been collected. In Eq. 10, collision-free position and desired velocity have been formulated. In the equation, the combination of the current position ($\mathbf{P}_{i,k}$) and current velocity ($\upsilon_{i,k}$) with sampling time (Δt) gives the next step (k) of position

$$\mathbf{P}_{i,k+1} = \mathbf{P}_{i,k} + \Delta t.\upsilon_{i,k} \tag{10}$$

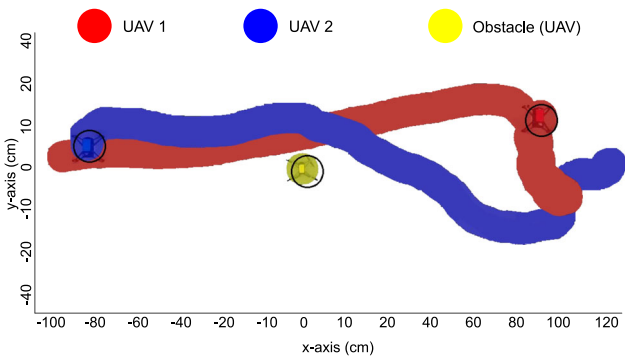

Fig. 12 The RVO results for UAVs in real-time

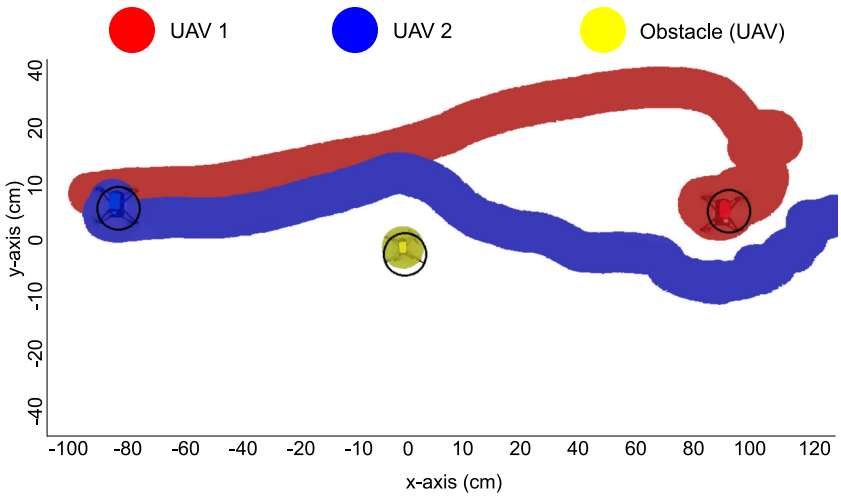

Fig. 13 The HRVO results for UAVs in real-time

for each agent/UAV (i). Therefore, the algorithm is able to compare collision-free trajectories for each VO avoidance approach.

In Figs. 11, 12, 13, and 14, red and blue UAVs have shown cooperative working, and yellow UAV has not interacted with blue and red UAVs. Other specific information is black circles. Black circles show the position of the UAVs with noises. That means the system does not know the exact position of the UAVs. Lastly, to employ FIMVO, K_s^1 and K_s^2 scaling factors have been defined as 1563 mm 750 mm, respectively.

In Fig. 11, applied VO results have been seen as a real-time system. All approaches have been tested ten times, and one of them has been chosen randomly. This figure shows the collision, which is expected because of noises and uncertain parameters in a real-time system. Considering the algorithm processing, the VO approach is the fastest compared with others-total task performance time 9.15 sec.

The RVO is safer than the VO approach, and the simulation results prove it. In real-time tests, this information shows the same result as the simulation. It shows safer and slower processing than VO in Fig. 12. Total task performance time 12.35 sec.

In Fig. 13, HRVO shows good cooperative and non-cooperative working in terms of reliability. It has the safest approach when compared with traditional and proposed obstacle avoidance approaches. However, computation time is a problem for real-time applications. Total task performance time has been measured at 15.25 sec.

In Fig. 14, the proposed approach results can be seen. It is faster than HRVO and safer than RVO. FIMVO scrutinize the capability of the system performance and reliability. At this point, it shows novelty. When compared with VO, RVO, and HRVO, FIMVO has 11.35 sec total time.

In Table 3, total test results of obstacle avoidance in multiple UAV real-time applications have been represented. In the real-time tests, the total collision counts, and the mean of task performance times have been investigated. The results show that FIMVO has the best in terms of collision with obstacles; also, when the averages of their task performances are considered, it is seen that RVO and FIMVO have almost the

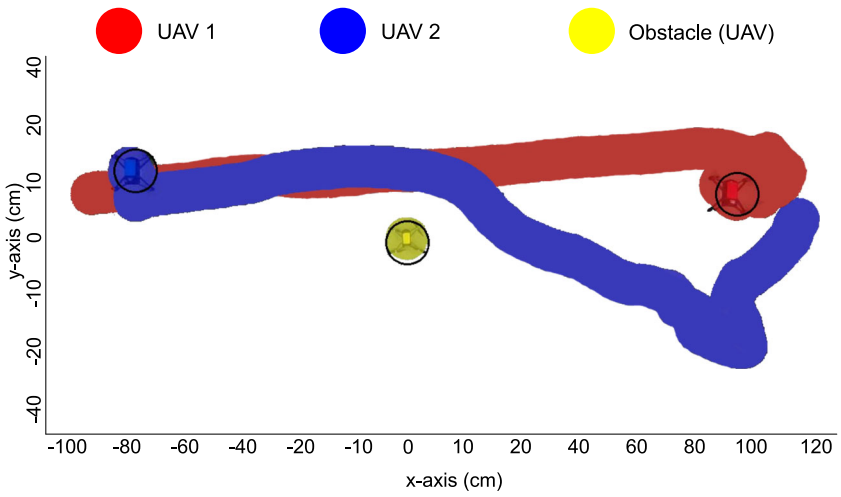

Fig. 14 The FIMVO results for UAVs in real-time

Table 3 Total real-time test results

Approach	Total collision counts	Mean of task performance time (s)
VO	6	9.08
RVO	3	12.48
HRVO	1	16.01
FIMVO	0	12.33

same completion times. However, HRVO shows the slowest results even though it has considerable collision avoidance counts, such as 9 avoidance out of 10.

If we evaluate each result in a performance graph in terms of reliability, trajectory smoothness, task performance and computation simplicity, the results of the compared and proposed approaches are seen in Fig. 15. The performance results of the proposed and compared avoidance approaches come from ten times real-time testing, independently. The results have been scaled between $[0, 1]$. It is observed that the reliability of the system is closely linked with the collision counts, with trajectory smoothness representing the first derivative of the warning zone trajectory road. Task performance, focusing on goal attainment, constitutes another crucial parameter. The final parameter, the computation simplicity, directly correlates with the computation time for each cycle. Notably, trajectory smoothness holds particular significance in Multi-Agent Systems (MAS) as, without a smooth trajectory, controllers in each agent/UAV must contend with manoeuvring effects to ensure stability. Consequently, employing a classical controller structure can lead to a smoother trajectory resolution for MAS and multiple UAVs.

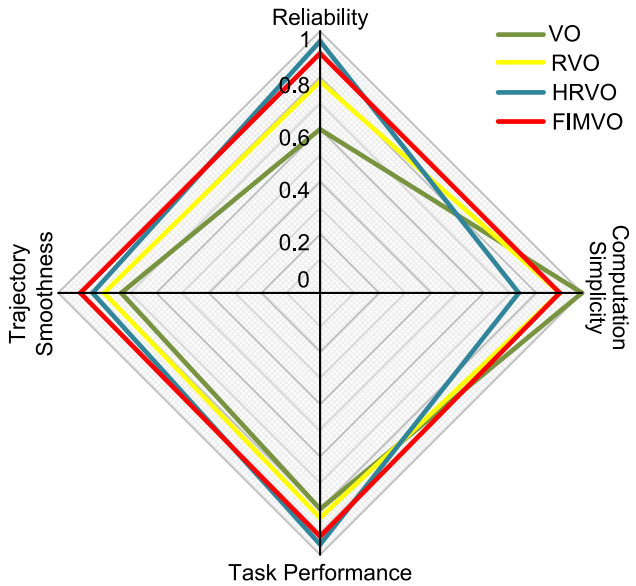

Fig. 15 Performance results

In the performance result figure, each performance index has been calculated over N real-time experiments ($N = 10$) for the proposed and compared velocity obstacle avoidance approach. The performance indices have been calculated as given below:

1. Reliability = $(N - C)/N$. Here, C represents the number of collisions in all experiments.
2. Trajectory smoothness performance index value has been calculated using the first derivative of the trajectory path at the point where collision cone and warning zone are intersected. It is noted that the warning zone radius has been selected as $r = 7cm$.
3. Task performance = S/N. In the equation, S represents the number of successful arrivals to the target out of N number of experiments.
4. Computation simplicity is calculated using the mean of the performance time, given in Table 3, and scaled in between $[0 - 1]$.

The VO algorithm stands out as the fastest among the considered algorithms. However, its applicability falls short when considering various comparison parameters for all applications. In terms of reliability, the HRVO approach yields the best results, as depicted in Fig. 15. Our proposed FIMVO approach excels in trajectory smoothness. When assessing task performance, FIMVO and HRVO exhibit nearly identical results. The performance of the RVO aligns as intermediate in terms of reliability, trajectory tracking, and task performance when compared to other algorithms. The proposed FIMVO approach integrates VO, RVO, and HRVO approaches using fuzzy logic, resulting in enhanced reliability and superior trajectory smoothness compared to RVO and HRVO. Furthermore, it demonstrates comparable task performance to HRVO.

5 Conclusions and Future Work

In this study, fuzzy interacting multiple-model velocity obstacle FIMVO avoidance has been proposed as a new approach for swarm and multi-agent systems. The proposed approach has been compared with three different geomet-

ric approaches based on velocity obstacles. For comparison, simulation and real-time experiments have been tested ten times independently. For the real-time system, three UAVs were used as cooperative and non-cooperative. Moreover, these UAVs had the same controller structure and parameters. The test results were investigated in terms of trajectory smoothness, task performance, algorithm simplicity, and reliability. Performance criteria showed that FIMVO had a better smooth trajectory and better algorithm simplicity than HRVO, and also, taking into account reliability, it was faster than RVO and VO.

The proposed approach will be tested with ten UAVs and different scenarios in future works. Moreover, different velocity obstacle avoidance approaches, such as optimal reciprocal velocity obstacle avoidance or generalised velocity obstacle avoidance approaches, will be combined with FIMVO. To increase the challenge in real-time, different noises will be added to the measurement part, and these noises can be extremely heavy-tailed non-Gaussian distributions. Lastly, the FIMVO approach will be investigated by different intelligent controllers, and then stability analysis will be chosen as another performance criterion for FIMVO and the compared approaches.

Appendix A: Simulation Results with Multiple Agents

These results demonstrate that the proposed collision avoidance algorithm achieves a comparable performance as in the case of three UAVs.

In this Appendix presents simulation results from the proposed and compared methods with multi-agents, 14 agents in the considered example. The sampling time has been selected and fixed as 0.05s. Then, 1000 time tests independently with multi-agents have been shown in Table 4, and also, in Fig. 16, one of the tested results has been represented.

Table 4 Total 1000 Monte-Carlo simulation test results

Method	Total collision counts	Mean of task performance time (s)
VO	971	8.58
RVO	524	13.67
HRVO	259	15.64
FIMVO	195	11.73

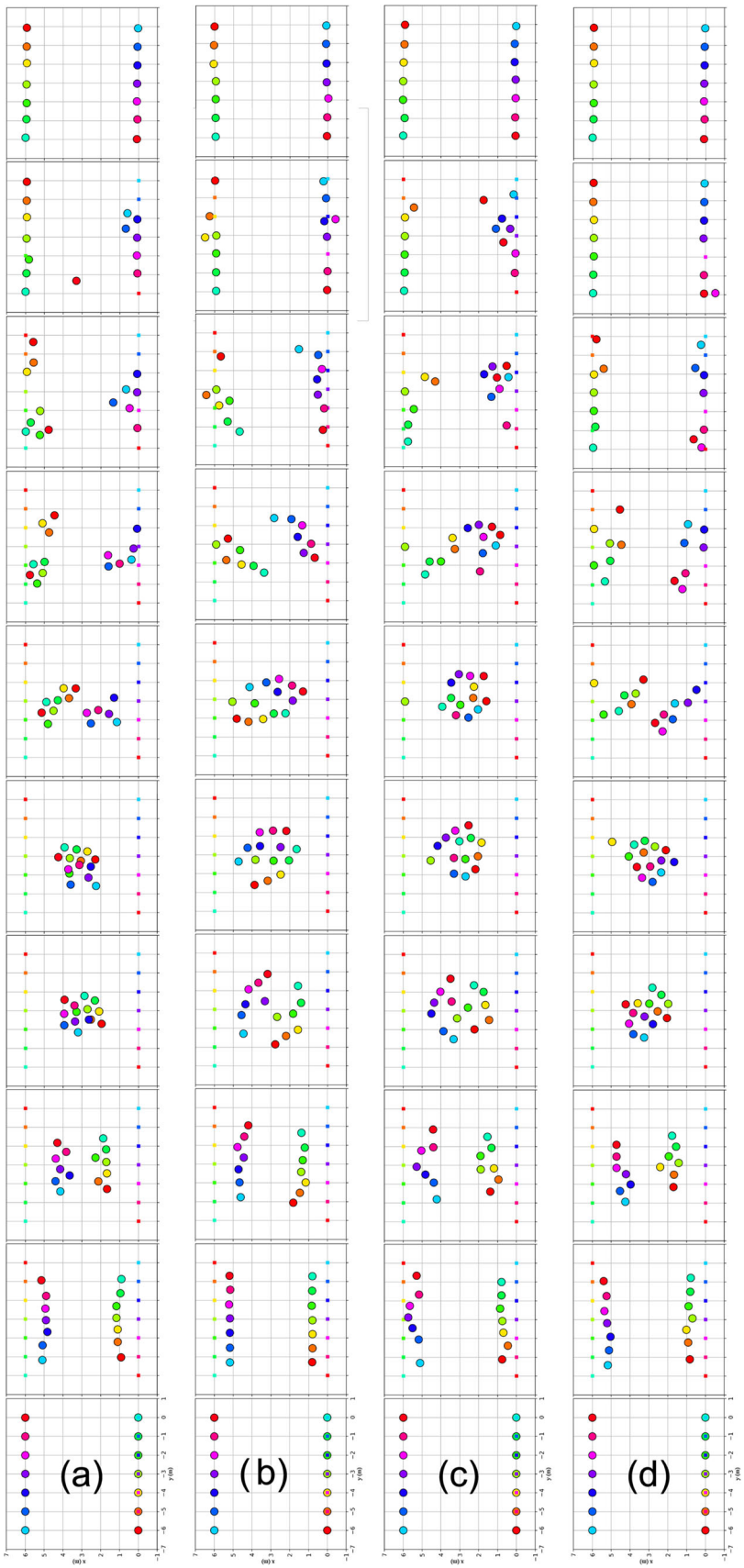

Fig. 16 (a) VO, (b) RVO, (c) HRVO, (d) FIMVO avoidance approaches' results

Acknowledgements We acknowledge the Turkish government for funding the doctoral scholarship of Fethi Candan.

Author Contributions Conceptualization, methodology, software, F. Candan; Validation, F. Candan and A. Beke; writing–original draft preparation, F.Candan, L. Mihaylova and M.Mahfouf; writing–review and editing F.Candan, L. Mihaylova and M.Mahfouf. All authors have read and agreed to the published version of the manuscript.

Funding This research received no external funding.

Data Availability Statement Not applicable.

Declarations

Institutional Review Board Statement Not applicable.

Informed Consent Statement Not applicable.

Conflicts of Interest The authors declare no conflict of interest.

References

1. Barnard, J.: Use of unmanned air vehicles in oil, gas and mineral exploration activities. In: AUVSI Unmanned Systems North America Conference, Denver, CO, USA (2010)
2. Nigam, N.: The multiple unmanned air vehicle persistent surveillance problem: a review. Machines **2**(1), 13–72 (2014)
3. Al-Younes, Y.M., Al-Jarrah, M.A., Jhemi, A.A.: Linear vs. nonlinear control techniques for a quadrotor vehicle. In: 7th International Symposium on Mechatronics and Its Applications, pp. 1–10. IEEE (2010)
4. Argentim, L.M., Rezende, W.C., Santos, P.E., Aguiar, R.A.: PID, LQR and LQR-PID on a quadcopter platform. In: 2013 International Conference on Informatics, Electronics and Vision (ICIEV), pp. 1–6. IEEE (2013)
5. Candan, F., Beke, A., Kumbasar, T.: Design and deployment of fuzzy PID controllers to the nano quadcopter Crazyflie 2.0. In: 2018 Innovations in Intelligent Systems and Applications (INISTA), pp. 1–6. IEEE (2018)
6. Şahin, İ, Ulu, C.: Altitude control of a quadcopter using interval type-2 fuzzy controller with dynamic footprint of uncertainty. ISA Trans. **134**, 86–94 (2023)
7. Zhao, W., Go, T.H.: Quadcopter formation flight control combining mpc and robust feedback linearization. J. Frankl. Inst. **351**(3), 1335–1355 (2014)
8. Niculescu, V., Lamberti, L., Palossi, D., Benini, L.: Automated tuning of end-to-end neural flight controllers for autonomous nano-drones. In: 2021 IEEE 3rd International Conference on Artificial Intelligence Circuits and Systems (AICAS), pp. 1–4. IEEE (2021)
9. Niculescu, V., Lamberti, L., Conti, F., Benini, L., Palossi, D.: Improving autonomous nano-drones performance via automated end-to-end optimization and deployment of dnns. IEEE J. Emerg. Sel. Top. Circuits Syst **11**(4), 548–562 (2021)
10. Zhao, Y., Zheng, Z., Liu, Y.: Survey on computational-intelligence-based UAV path planning. Knowl-based Syst **158**, 54–64 (2018)
11. Suzuki, M., Uchiyama, K., Bennet, D., MacInnes, C.: Three-dimensional formation flying using bifurcating potential fields. In: AIAA Guidance, Navigation, and Control Conference, p. 5884 (2009)
12. Candan, F., Peng, Y., Mihaylova, L.: A comparison of obstacle dependant gaussian and hybrid potential field methods for collision avoidance in multi-agent systems. In: Proceedings of the 1st International Conference on Computing and Machine Intelligence (ICMI 2021). Sheffield (2021)
13. Douthwaite, J.A., Zhao, S., Mihaylova, L.S.: A comparative study of velocity obstacle approaches for multi-agent systems. In: Proceedings of the UKACC 12th International Conference on Control (CONTROL), pp. 289–294. IEEE (2018)
14. Douthwaite, J.A., Zhao, S., Mihaylova, L.S.: Velocity obstacle approaches for multi-agent collision avoidance. Unmanned Syst. **7**(01), 55–64 (2019)
15. Jenie, Y.I., Van Kampen, E.-J., de Visser, C.C., Chu, Q.P.: Selective velocity obstacle method for cooperative autonomous collision avoidance system for unmanned aerial vehicles. In: AIAA Guidance, Navigation, and Control (GNC) Conference, p. 4627 (2013)
16. Alonso-Mora, J., Beardsley, P., Siegwart, R.: Cooperative collision avoidance for nonholonomic robots. IEEE Trans. Robot. **34**(2), 404–420 (2018)
17. Douthwaite, J.A., De Freitas, A., Mihaylova, L.S.: An interval approach to multiple unmanned aerial vehicle collision avoidance. In: Proceedings of the Sensor Data Fusion: Trends, Solutions, Applications (SDF), pp. 1–8 (2017). IEEE
18. Jenie, Y.I., van Kampen, E.-J., de Visser, C.C., Ellerbroek, J., Hoekstra, J.M.: Three-dimensional velocity obstacle method for uncoordinated avoidance maneuvers of unmanned aerial vehicles. J. Guid. Control Dyn. **39**(10), 2312–2323 (2016)
19. Xiuxia, Y., Yi, Z., Weiwei, Z.: Obstacle avoidance method of three-dimensional obstacle spherical cap. J. Syst. Eng. Electron. **29**(5), 1058–1068 (2018)
20. Snape, J., Van Den Berg, J., Guy, S.J., Manocha, D.: The hybrid reciprocal velocity obstacle. IEEE Trans. Robot. **27**(4), 696–706 (2011)
21. Fiorini, P., Shiller, Z.: Motion planning in dynamic environments using velocity obstacles. Int. J. Robot. Res. **17**(7), 760–772 (1998)
22. Van den Berg, J., Lin, M., Manocha, D.: Reciprocal velocity obstacles for real-time multi-agent navigation. In: 2008 IEEE International Conference on Robotics and Automation, pp. 1928–1935. IEEE (2008)
23. Snape, J., Van Den Berg, J., Guy, S.J., Manocha, D.: Independent navigation of multiple mobile robots with hybrid reciprocal velocity obstacles. In: 2009 IEEE/RSJ International Conference on Intelligent Robots and Systems, pp. 5917–5922. IEEE (2009)
24. Beke, A., Kumbasar, T.: Type-2 fuzzy logic-based linguistic pursuing strategy design and its deployment to a real-world pursuit evasion game. IEEE Trans. Cybern. **50**(1), 211–221 (2018)
25. Zhang, D., Wang, J.: Fuzzy PID speed control of BLDC motor based on model design. In: Journal of Physics: Conference Series, vol. 1303, p. 012124. IOP Publishing (2019)
26. Python3. http://www.python.org/. Accessed 14 Sep 2022 (2015)
27. DJI Tello EDU. https://m.dji.com/uk/product/tello-edu/. Accessed 14 Sep 2022 (2023)

28. Sarabakha, A., Fu, C., Kayacan, E., Kumbasar, T.: Type-2 fuzzy logic controllers made even simpler: from design to deployment for UAVs. IEEE Trans. Ind. Electron. **65**(6), 5069–5077 (2017)
29. Guzay, C., Kumbasar, T.: Aggressive manoeuvring of a quadcopter via differential flatness-based fuzzy controllers: from tuning to experiments. Appl. Soft Comput. **126**, 109223 (2022)
30. Intel Realsense. https://www.intelrealsense.com/stereo-depth/. Accessed 14 Sep 2022 (2023)
31. Chen, B., Liu, X., Zhao, H., Principe, J.C.: Maximum correntropy Kalman filter. Automatica **76**, 70–77 (2017)
32. Fan, X., Wang, G., Han, J., Wang, Y.: Interacting multiple model based on maximum correntropy Kalman filter. IEEE Trans. Circuits Syst. II Express Briefs **68**(8), 3017–3021 (2021). https://doi.org/10.1109/TCSII.2021.3068221
33. Candan, F., Beke, A., Shen, C., Mihaylova, L.: An interacting multiple model correntropy Kalman filter approach for unmanned aerial vehicle localisation. In: Proceedings of the International Conference on INnovations in Intelligent Systems and Aplications (INISTA), pp. 1–6 (2022). https://doi.org/10.1109/INISTA55318.2022.9894214. IEEE
34. Shen, C., Mihaylova, L.: A flexible robust Student's t-based multimodel approach with maximum versoria criterion. Sig. Process. **182**, 107941 (2021)
35. Li, S., Li, L., Shi, D., Zou, W., Duan, P., Shi, L.: Multi-kernel maximum correntropy Kalman filter for orientation estimation. IEEE Robot. Autom. Lett. **7**(3), 6693–6700 (2022). https://doi.org/10.1109/LRA.2022.3176798

Fethi Candan received B.Sc. degrees in Electrical & Electronics and Mechanical & Manufacturing Engineering between 2011-2016, from Bilecik S.E. University, Bilecik, Turkiye. His M.Sc. degree is in Control and Automation Engineering in 2018, Istanbul Technical University, Istanbul, Turkiye. He received his Ph.D. degree with the Automatic Control and Systems Engineering Department, Sheffield, United Kingdom. Currently, he is working at the University of Idaho as a postdoctoral fellow at the Department of Mechanical Engineering and Soil & Water Systems.

His research interests are in the areas of control theory, state estimation, unmanned air vehicles, swarm, intelligent systems, and their real-world applications.

Aykut Beke received his B.Sc., M.Sc. and Ph.D. degrees in Control and Automation Engineering from the Istanbul Technical University in 2015, 2018 and 2023, respectively. He is currently working as a senior control system design engineer at ASELSAN Inc., Turkey.

He has currently authored more than 20 papers in international conferences and journals. His research interests are in the areas of control theory, type-2 fuzzy logic, machine learning, deep learning, computational intelligence, and their real-world applications.

Mahdi Mahfouf received the M.Phil. and Ph.D. degrees in control systems from The University of Sheffield, Sheffield, U.K., in 1987 and 1991, respectively. Since 2005, he has held a Personal Chair in intelligent systems engineering with The University of Sheffield (UK). He is the author of more than 360 papers, out of which more than 140 are journal papers. He has worked in the area of intelligent systems engineering, with a strong emphasis on fuzzy systems, modelling, control, and optimization for more than 35 years, with special applications to industrial systems and biomedicine. During this period, he had received several awards and prizes for his seminal work.

Lyudmila Mihaylova With a wide experience on developing methods for knowledge extraction from data and introducing autonomy, including for unmanned aerial vehicles (UAVs), human-robot interactions, Prof. Lyudmila Mihaylova is leading a strong team with activities part of the Automatic Control and Systems Engineering (ACSE) and Sheffield Robotics at the University of Sheffield. Her expertise is in the areas of machine learning, autonomous systems: for sensing, tracking, navigation, decision making and with a variety of data from optical, thermal images, radar, LiDAR sensors, wireless networks and others. With her team she develops research methods that are able to quantify the impact of uncertainties, especially from the sensor data, environment, system dynamics and other factors influencing AI solutions.

She is Associate Editor-in-Chief for the IEEE Transactions on Aerospace and Electronic Systems, Senior Editor for the Target Tracking and Multi-sensor data Fusion area since 2021, and a Subject Area Editor for the Elsevier Signal Processing Journal since 2022. She is a guest Editor for a special issue for Frontiers of Robotics and AI (2022023). She won the Tammy Blair best award from the International Conference of Information Fusion 2017, best paper awards from the IEEE DESSERT'2019, 17th IEEE SPA'2013 Conference and IEEE Sensor Data Fusion Workshop, 2013, best student paper award from IEEE MFI 2021, IEEE ICMA' 2023 and others. She was the president of the International Society of Information Fusion (ISIF) from 2017 to 2018. She is on the Board of Directors of ISIF. She has been serving for organising conferences – as the general vice chair of UKCI'2022, a program chair for the International Conference on Information Fusion, Fusion 2022, technical chair for Fusion 2021, publicity chair for IEEE MFI' 2021 and UKCI 2021. She was the general vice-chair for the International Conference on Information Fusion 2018 (Cambridge, UK), of the IET Data Fusion & Target Tracking 2014 and 2012 Conferences, publications chair for ICASSP 2019 (Brighton, UK) and others.